

# Increased fractional anisotropy in the motor tracts of Parkinson's disease suggests compensatory neuroplasticity or selective neurodegeneration

Jilu Princy Mole<sup>1,2,5</sup> · Leena Subramanian<sup>1,2,5</sup> · Tobias Bracht<sup>1,3</sup> · Huw Morris<sup>4</sup> · Claudia Metzler-Baddeley<sup>1</sup> · David E. J. Linden<sup>1,2,5</sup>

Received: 19 August 2015 / Revised: 15 October 2015 / Accepted: 27 October 2015 / Published online: 15 January 2016  
© The Author(s) 2016. This article is published with open access at Springerlink.com

## Abstract

**Objective** To determine the differences in motor pathways and selected non-motor pathways of the basal ganglia in Parkinson's disease (PD) patients compared to healthy controls (HCs).

**Methods** We analysed diffusion weighted imaging data of 24 PD patients and 26 HCs. We performed deterministic tractography analysis using the spherical deconvolution-based damped Richardson-Lucy algorithm and subcortical volume analysis.

**Results** We found significantly increased fractional anisotropy (FA) in the motor pathways of PD patients: the bilateral corticospinal tract (right; corrected  $p=0.0003$ , left; corrected  $p=0.03$ ), bilateral thalamus-motor cortex tract (right; corrected  $p=0.02$ , left; corrected  $p=0.004$ ) and the right supplementary area-putamen tract (corrected  $p=0.001$ ). We also

found significantly decreased FA in the right uncinate fasciculus (corrected  $p=0.01$ ) and no differences of FA in the bilateral supero-lateral medial forebrain bundles ( $p>0.05$ ) of PD patients compared to HCs. There were no subcortical volume differences ( $p>0.05$ ) between the PD patients and HCs. **Conclusion** These results can inform biological models of neurodegeneration and neuroplasticity in PD. We suggest that increased FA values in the motor tracts in PD may reflect compensatory reorganization of neural circuits indicative of adaptive or extended neuroplasticity.

## Key points

- Fractional anisotropy was higher in motor pathways of PD patients compared to healthy controls.
- Fractional anisotropy was lower in the uncinate fasciculus of PD patients compared to healthy controls.
- Increased fractional anisotropy could suggest adaptive neuroplasticity or selective neurodegeneration.

**Electronic supplementary material** The online version of this article (doi:10.1007/s00330-015-4178-1) contains supplementary material, which is available to authorized users.

✉ David E. J. Linden  
lindend@cardiff.ac.uk

**Keywords** Deterministic tractography · Parkinson's disease · Neuroplasticity · Diffusion-weighted imaging · Fractional anisotropy

- <sup>1</sup> Cardiff University Brain Research Imaging Centre (CUBRIC), School of Psychology, Cardiff University, Cardiff, UK
- <sup>2</sup> Institute of Psychological Medicine and Clinical Neurosciences (IPMCN), School of Medicine, Cardiff University, Cardiff, UK
- <sup>3</sup> Department of Psychiatry, University of Bern, Bern, Switzerland
- <sup>4</sup> Department of Clinical Neurology, Institute of Neurology, University College London, London, UK
- <sup>5</sup> MRC Centre for Neuropsychiatric Genetics and Genomics, School of Medicine, Cardiff University, Hadyn Ellis Building, Maindy Road, Cathays, Cardiff CF24 4HQ, UK

## Abbreviations

AD	Axial diffusivity
CST	Corticospinal tract
dRL	Damped Richardson-Lucy
FA	Fractional anisotropy
PD	Parkinson's disease
sIMFB	Supero-lateral medial forebrain bundle
SMA-PUT	Supplementary motor area-putamen tract
THAL-MC	Thalamus-motor cortex tract
UNF	Uncinate fasciculus

## Introduction

Because the motor symptoms of Parkinson's disease (PD) only arise after approximately 80 % depletion of striatal dopamine, it has long been thought that compensatory plasticity must occur both within and outside the basal ganglia as the pathology progresses [1]. Such compensatory processes, as well as any long-range deficits arising from degeneration of the basal ganglia pathways, should ultimately be reflected in the architecture of the fibre tracts connecting motor cortex, basal ganglia and thalamus.

To date most diffusion-based studies on PD have only considered changes within defined regions of interest (ROIs) in grey matter [2] or whole brain voxel-wise analysis of white matter using tract-based spatial statistics (TBSS) [3]. These approaches are prone to partial volume effects and entail difficulties of spatial alignment across participants. Given that there are crossing fibres in about 90 % of the voxels of the brain, allocation of voxel-based findings to specific tracts can be highly speculative [4]. To overcome these limitations, we conducted deterministic tractography using the damped Richardson-Lucy (dRL) algorithm which is more sensitive to detect group differences than voxel-based approaches and produces anatomically plausible white matter tracts [4]. This method improves fibre tracking in areas of complex fibre architecture and regions affected by partial volume [5].

We reconstructed the following motor pathways: (i) the corticospinal tract, (ii) fibre connections between the thalamus and the motor cortex, and (iii) fibre connections between the supplementary motor area and the putamen. The corticospinal tract is crucial for self-initiated movements and thus putatively involved in bradykinesia in PD [6]. Post-mortem and diffusion studies show direct white matter fibre connections from the supplementary motor area to the striatum [7]. It is assumed that these connections are relevant for motor performance in PD [8]. The thalamus, a relay centre for sensory and motor information, conveys motor inputs from the basal ganglia to the cortex and decreased dopaminergic innervation to the thalamus is assumed to contribute to the pathophysiology of PD

[9]. These tracts are thus closely related to PD pathophysiology and symptoms, and potentially also to their remediation. We were also interested in potential changes in the non-motor tracts of (iv) the uncinate fasciculus and (v) the supero-lateral medial forebrain bundle. The uncinate fasciculus is assumed to be involved in language, emotional processing and episodic memory [10], while the supero-lateral medial forebrain bundle mediates reward-seeking [11], which are also potentially affected in PD. Hence our objective was to determine the differences in motor pathways and selected non-motor pathways of the basal ganglia in PD patients compared to healthy controls (HCs). Additionally we wanted to determine whether there were any group differences in basal ganglia volumes that could drive potential group differences in the white matter measures, therefore we also performed subcortical volume analysis [12].

## Materials and methods

### Participants

Twenty-six PD patients in Hoehn and Yahr stages I-III were recruited from clinics in South Wales by H.M. and collaborating clinicians (see Acknowledgements). They were scanned before and after taking part in a trial that compared functional magnetic resonance imaging (fMRI)-based neurofeedback and exercise with a gaming console over 12 weeks (NCT01867827) and will be reported elsewhere. Here we use the data from the baseline scan, which were unaffected by the intervention. The study was approved by the local NHS research ethics committee, and all patients gave informed consent. Diffusion MRI data of 26 HCs from a previous study into the effects of ageing on white matter microstructure [13] which used the same diffusion imaging protocol as the current study were included to provide an age-matched healthy comparison group (Table 1). Two PD patients' scans were excluded from the final analysis due to corrupted data files.

**Table 1** Demographics of the Parkinson's disease (PD) patients and healthy controls (HCs)

Demographic	PD patients (n = 24)	HCs (n = 26)	Analyses
Age	63.42 ± 10.82	64.88 ± 8.06	P = 0.5918, Two sample t-test
Sex (M:F)	22:2	17:9	P = 0.06, Chi squared test
Handedness (R:L)	20:4	24:2	P = 0.3293, Chi squared test
H and Y Stage	1.75 ± 0.47	NA	-
UPDRS score	25.04 ± 11.01	NA	-
MOCA	26.54 ± 2.01	NA	-
LEDD (mg)	537.64 ± 340.69	NA	-

*MOCA* The Montreal Cognitive Assessment, *H and Y* Hoehn and Yahr stage, *UPDRS* Unified Parkinson's Disease Rating Scale (pre-intervention and off medication), *LEDD* Levodopa Equivalent Daily Dose, *M* male, *F* female, *R* right, *L* left

## Magnetic resonance (MR) data acquisition

Diffusion weighted MRI data were acquired on the 3T GE Signa HDx system (General Electric Healthcare) in Cardiff University Brain Research and Imaging Centre (CUBRIC) using a peripherally gated twice-refocused pulse-gradient spin-echo echo-planar imaging sequence providing whole oblique axial (parallel to the commissural plane) brain coverage. Data were acquired from 60 slices of 2.4-mm thickness, with a field of view (FOV) of 23 cm, and an acquisition matrix of  $96 \times 96$  (yielding isotropic voxels of  $2.4 \times 2.4 \times 2.4$  mm, reconstructed to a resolution of  $1.9 \times 1.9 \times 2.4$  mm). Echo time (TE) was 87 ms and parallel imaging (ASSET factor=2) was used. Diffusion encoding gradients ( $b=1,200$  s/mm<sup>2</sup>) were applied along 30 isotropically-distributed directions [14] as the optimal b-value for deriving good estimates of fractional anisotropy (FA), mean diffusivity (MD) and fibre orientation is 750–1,300 s/mm<sup>2</sup> [15, 16].

T1-weighted structural scans were acquired using an oblique-axial, 3D fast spoiled gradient recalled sequence (FSPGR) with the following parameters: 178 slices; TE=3 ms, TR=7.9 ms, voxel size  $1.0 \times 1.0 \times 1.0$  mm<sup>3</sup>,  $256 \times 256$  FOV. These structural images were acquired for co-registration and anatomical localization of regions of interest for the tracts. These FSPGR images were also used as a template to draw ROIs for the virtual dissection of the tracts and for the subcortical volumes analyses.

## Diffusion MR Imaging (MRI) data processing

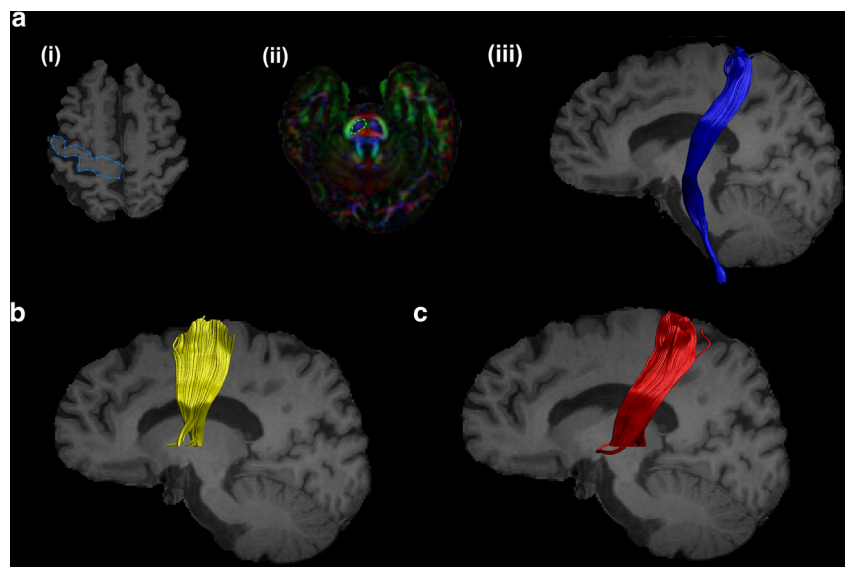
The diffusion MRI data were corrected for subject motion, echo planar imaging (EPI) distortions and Eddy Current (EC) distortions in ExploreDTIv4.8.3 [17]. We performed an

affine registration to the non-diffusion-weighted images, with appropriate re-orienting of the encoding vectors [18]. A single diffusion tensor model was fitted [19] to the data in order to compute the quantitative parameters: FA, MD, radial and axial diffusivity (RD and AD). The fibre orientation density function (fODF) was estimated with the dRL algorithm in each voxel [5]. Data were also corrected for cerebrospinal fluid (CSF)-based partial volume artefacts using the Free Water Elimination (FWE) method [20]. The rationale for this correction was that ageing and neurodegeneration are associated with grey and white matter tissue loss, and CSF-based partial volume effects have been shown to lead to artificial decreases in FA and increases in MD.

## Deterministic tractography

Whole brain dRL-based deterministic tractography was performed in ExploreDTIv4.8.3 [17] using the spherical deconvolution-based dRL algorithm following peaks in the fODF reconstructed from dRL [4, 5]. The dRL algorithm preserves angular resolution and reduces the number of false positive fibre orientations. For each voxel in the data set, streamlines were initiated along any peak in the fODF that exceeded an amplitude of 0.05. This enables multiple fibre pathways to be generated from any voxel. Each streamline was continued in 0.5 mm steps following the peak in the ODF that subtended the smallest angle to the incoming trajectory. The termination criterion was set to an angle threshold greater than 45°, thus streamlines that had angles above this threshold were excluded from the final tracts. Three-dimensional fibre reconstructions were obtained by applying waypoint ROI gates (“AND”, “OR” and “NOT” gates

**Fig. 1** Reconstructed motor tracts. **(a)** Corticospinal tract: (i) Axial slice of T1 image showing “SEED” region. (ii) Axial slice of FA image showing “AND” region. (iii) Sagittal slice of T1 image showing the reconstructed CST. **(b)** Reconstructed supplementary area-putamen tract and **(c)** thalamus-motor cortex tract on sagittal slices of T1 image



following Boolean logic) to isolate specific tracts from the whole brain tractography data.

#### Corticospinal tract (CST)

For the segmentation of the CST, the primary motor cortex was identified in the axial slice of a T1 image using a “SEED” region (in blue) (Fig. 1a (i)). Further, an “AND” region (in green) was drawn in the brain stem (identified as the blue colour of the pons in the anterior part of the brain stem) in the axial slice of an FA image (Fig. 1a (ii)). The CST of a representative subject on a sagittal slice of a T1 image is shown in (Fig. 1a (iii)).

#### Thalamus-motor cortex (THAL-MC) and supplementary area-putamen (SMA-PUT) tracts

The ROIs for segmentation of THAL-MC and SMA-PUT tracts were derived by creating masks chosen from the AAL (Anatomical Automatic Labelling) atlas in the MNI (Montreal Neurological Institute) space. These masks were warped to the individual native space of each subject using inverse parameters derived from warping the T1 image to the AAL template. These masks were then used as “SEED” and “AND” regions in *ExploreDTI* for segmenting out the respective tracts. Unwanted regions and spurious tracts were removed by using the “NOT” gate. The final SMA-PUT and THAL-MC tracts in a sagittal slice of a T1 image of a representative subject are shown in Fig. 1b and c, respectively.

#### Uncinate fasciculus (UNF)

For segmentation of the UNF, the most posterior slice in the coronal view of a T1 image where the frontal and the temporal lobes are separated was chosen. The “SEED” region (in blue)

was drawn around the temporal lobe (Fig. 2d (i)) and the “AND” region (in green) was drawn around the basal forebrain (Fig. 2d (ii)). The UNF tract of a representative subject on a sagittal slice of a T1 image is shown in (Fig. 2d (iii)).

#### Supero-lateral medial forebrain bundle (slMFB)

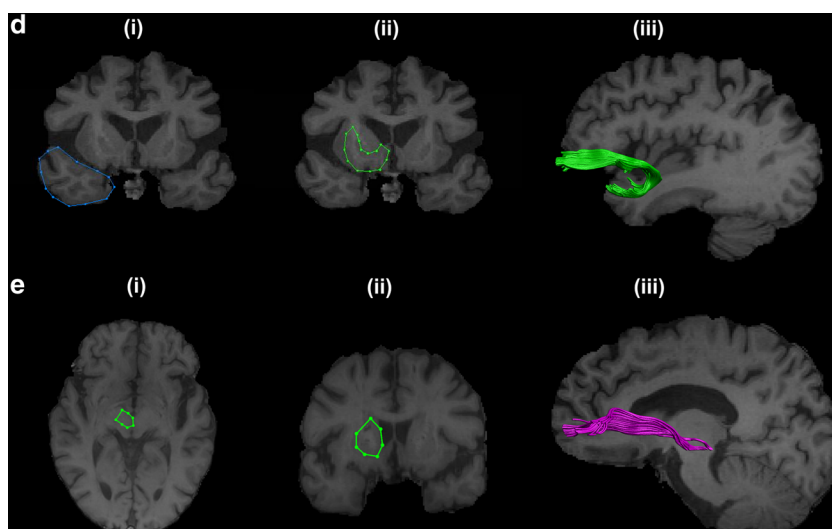
For reconstruction of the slMFB one horizontal “AND” region was placed surrounding the ventral tegmental area. The anatomical borders for this AND region were laterally the substantia nigra, anteriorly the mammillary bodies and posteriorly the red nucleus (Fig. 2e (i)). Another “AND” region was drawn surrounding the caudate and putamen on a coronal section at the height of the nucleus accumbens (Fig. 2e (ii)) [21]. The slMFB tract of a representative subject on a sagittal slice of a T1 image is shown in (Fig. 2e (iii)).

Each reconstructed tract was visually inspected and any obvious outlier streamlines that were not consistent with their known anatomy were excluded by drawing “NOT” regions and the entire procedure was performed separately for both hemispheres.

#### Subcortical volumes

We measured volumes of subcortical brain structures using FSL's FIRST software (FMRIB Image Registration and Segmentation Tool) [12]. The structures of the thalamus, caudate, putamen, pallidum, hippocampus, amygdala, nucleus accumbens and ventricles were extracted for both hemispheres and their volumes measured for all T1-weighted MR images of the PD patients and HCs. The extracted volumes were normalized using the scaling factor obtained from brain tissue normalization for subject head size, using SIENAX (Structural Image Evaluation using Normalization of Atrophy) [22].

**Fig. 2** Reconstructed non-motor tracts. **(d)** Uncinate fasciculus tract: (i) Coronal slice of T1 image showing “SEED” region for uncinate fasciculus segmentation. (ii) Coronal slice of T1 image showing “AND” region. (iii) Sagittal slice of T1 image showing reconstructed uncinate fasciculus tract. **(e)** Supero-lateral medial forebrain bundle: (i) Axial slice of T1 image showing “AND” region. (ii) Coronal slice of T1 image showing “AND” region. (iii) Sagittal slice of T1 image showing reconstructed supero-lateral medial forebrain bundle





## Statistical analysis

All the statistical analyses were carried out in the R statistical software v2.15.3 [23]. Before data analysis, all variables were checked for Gaussian distribution using the Shapiro-Wilk test ( $p < 0.05$ ) and were transformed using appropriate transformations if necessary.

We performed multivariate analyses of covariance (MANCOVAs) in each hemisphere for each of the five tracts separately with FA, MD, AD and RD as dependent variables and group (PD and HC) as independent variable, along with age and gender as covariates. These analyses were corrected for multiple comparisons using Bonferroni correction with a corrected threshold of  $p < 0.05$  ( $0.05/10 = 0.005$ ). Significant results were further analysed using post-hoc univariate ANOVAs also corrected for multiple comparisons using Bonferroni correction with a corrected threshold of  $p < 0.05$  ( $0.05/32 = 0.00156$ ). The inter-rater reliability of diffusion tensor indices derived from the manually reconstructed tracts was investigated using the inter-class correlation coefficient (ICC).

For the subcortical volumes analysis, we performed two sample t-tests comparing the corrected subcortical volumes of the PD patients and HCs.

We also extracted additional tractography measures of the number of reconstructed streamlines, number of voxels occupied by tract, tract volume and tract length for tracts with significant results from the MANCOVA also corrected for multiple comparisons using Bonferroni correction with a corrected threshold of  $p < 0.05$  ( $0.05/32 = 0.00156$ ).

The results of a complementary TBSS analysis are reported in the [Supplementary material](#).

## Results

In all PD patients and HCs, we obtained reliable reconstruction results of all investigated fibre tracts (Supplementary Table 1).

PD patients showed significantly higher FA in the motor (CST, SMA-PUT and THAL-MC) tracts but not in the non-motor (UNF and sIMFB) tracts. These effects were statistically supported by significant multivariate effects for group, followed up by the relevant significant univariate effects.

### Multivariate effects

The MANCOVAs demonstrated a significant effect of group (PD and HC) on the multivariate diffusion tensor indices (FA, MD, AD and RD) in the CST, SMA-PUT, THAL-MC and UNF, but not in the sIMFB (Table 2).

### Univariate group effects

Post-hoc analyses showed significantly increased FA and AD in right CST, and significantly increased FA in the left CST of the PD patients compared to HC (Table 3). In PD patients, there was significantly increased FA and AD in the right SMA-PUT tracts and significantly increased AD in the left SMA-PUT tracts. Similarly, there was significantly increased FA in both right and left THAL-MC tracts of the PD patients compared to HCs (Table 3). Conversely, in the UNF of PD patients, there was significantly decreased FA and significantly increased RD in the right UNF, and significantly increased MD in the left UNF (Table 3).

### Subcortical volumes analysis

We found no significant volume changes between PD patients and HCs in the FSL FIRST analysis of subcortical and ventricular volumes (Supplementary Table 3).

### Additional tractography measures

We found a significantly higher number of reconstructed streamlines, higher number of occupied voxels and larger tract volume in the tracts of PD patients compared to HCs (Supplementary Table 4).

## Discussion

Patients with early-stage PD relative to age-matched controls demonstrated a specific increase in FA and AD in the white matter of motor tracts which was not present for two non-motor comparison tracts.

In the previous literature, neurodegenerative disorders have generally been associated with decreased FA in the major pathways, which has been attributed to primary white matter degeneration, demyelination, reduced gliosis or axonal damage as a result of grey matter loss [24–26]. Diffusion tensor-based ROIs and whole brain analyses in PD have shown reduced FA or increased MD in a priori regions such as the substantia nigra and putamen [2, 3, 27]. Thus only our finding of decreased FA and increased RD in the UNF, but not our findings of increased FA and AD in the CST and cortico-basal ganglia tracts, would be compatible with a general neurodegenerative process.

### Neurodegenerative models

Our findings may reflect selective neurodegeneration. AD, which is the measure of diffusion in the principal fibre direction, is sensitive to the number of axons and their coherence [28] while RD, the measure of diffusion perpendicular to the

**Table 2** Multivariate effects

Tract		F statistic	Pillai's trace	P-value
Right CST	Group	F(4,43) = 4.6907	0.3	0.003132 ***
	Age	F(4,43) = 3.3356	0.23	0.018252
	Gender	F(4,43) = 3.1088	0.22	0.024736
Left CST	Group	F(4,43) = 8.5394	0.44	3.66E-05 ***
	Age	F(4,43) = 2.7190	0.2	0.04189
	Gender	F(4,43) = 2.5850	0.19	0.05026
Right SMA-PUT	Group	F(4,43) = 6.4230	0.38	0.000363 ***
	Age	F(4,43) = 10.5065	0.48	1.00E-05 ***
	Gender	F(4,43) = 0.5654	0.04	0.730037
Left SMA-PUT	Group	F(4,43) = 4.8551	0.31	0.002546 ***
	Age	F(4,43) = 5.5182	0.34	0.001123 ***
	Gender	F(4,43) = 0.3259	0.02	0.859045
Right THAL-MC	Group	F(4,43) = 4.7410	0.31	0.002939 ***
	Age	F(4,43) = 4.4941	0.29	0.00402 ***
	Gender	F(4,43) = 0.6916	0.06	0.601839
Left THAL-MC	Group	F(4,43) = 5.5699	0.34	0.001054 ***
	Age	F(4,43) = 4.4365	0.29	0.004326 ***
	Gender	F(4,43) = 1.4269	0.11	0.241373
Right UNF	Group	F(4,43) = 5.7824	0.28	0.002011 ***
	Age	F(4,43) = 2.5327	0.15	0.069178
	Gender	F(4,43) = 3.2413	0.18	0.030894
Left UNF	Group	F(4,43) = 5.0908	0.32	0.001898 ***
	Age	F(4,43) = 3.8483	0.26	0.009263
	Gender	F(4,43) = 2.6825	0.19	0.044023
Right sLMFB	Group	F(4,43) = 1.2095	0.1	0.320719
	Age	F(4,43) = 5.1433	0.32	0.001778 ***
	Gender	F(4,43) = 1.9735	0.15	0.115659
Left sLMFB	Group	F(4,43) = 1.1442	0.09	0.348703
	Age	F(4,43) = 4.3186	0.28	0.005032 ***
	Gender	F(4,43) = 3.2387	0.23	0.020777

\*\*\* = Bonferroni corrected  $p < 0.05$  ( $0.05/10 = 0.005$ )

*CST* corticospinal tract, *SMA-PUT* supplementary motor area-putamen tract, *THAL-MC* thalamus-motor cortex tract, *UNF* uncinate fasciculus, *sLMFB* supero lateral medial forebrain bundle

principal diffusion direction, is thought to reflect decreased myelination [29]. Therefore, in our data the results of elevated FA in combination with elevated AD could suggest selective neurodegeneration causing lower neural branching, decreases of axonal diameter and thus higher coherence along the principal orientation. Increased FA in these tracts may also occur as a primary pathogenic consequence of altered pallido-thalamic activity in PD. A combined diffusion tensor and histology-based study of rat model of traumatic brain injury showed that an increase in FA in the cortical regions was correlated with gliosis [30]. It has been suggested that FA is more related to axonal package density and less to myelination [31]. Along these lines, our data could suggest a higher axonal package density of motor pathways as there were no significant differences in RD in our cohort.

### Neuroplastic models

Alternatively, our findings might reflect early compensatory mechanisms associated with increases in axonal density in pathways of the cortico-basal-ganglia-thalamo-cortical loop. Such compensatory changes might preserve neural functions despite loss of the dopaminergic input [1]. A recent study in PD patients showed an increase in striato-cortical connectivity mediated by levodopa intake [32], hence it could also be suggested that increased FA in the SMA-PUT and THAL-MC tracts may be an adaptive response to abnormal dopaminergic modulation and levodopa intake.

Our results agree with the suggested compensation stages of PD where structures outside the basal ganglia, especially the SMA, would undergo change to counterbalance the

**Table 3** Univariate group effects on diffusion tensor indices of tracts between Parkinson's disease (PD) patients and healthy controls (HCs)

Tract	Diffusion tensor index	HC (n = 26) mean ± SD	PD (n = 24) mean ± SD	F statistic	p-value	Corrected p-value
Right CST	FA	0.54 ± 0.025	0.58 ± 0.024	F(1,48) = 24.32	1.02E-05	0.0003264 ***
	MD (1.0e-03)	0.71 ± 0.018	0.72 ± 0.032	F(1,48) = 2.601	0.1133	1
	RD (1.0e-03)	0.46 ± 0.022	0.45 ± 0.028	F(1,48) = 4.068	0.04932	1
	AD (1.0e-03)	1.21 ± 0.048	1.25 ± 0.072	F(1,48) = 16.24	0.000198	0.006336 ***
Left CST	FA	0.53 ± 0.027	0.56 ± 0.030	F(1,48) = 12.25	0.001017	0.032544 ***
	MD (1.0e-03)	0.72 ± 0.023	0.73 ± 0.024	F(1,48) = 2.098	0.154	1
	RD (1.0e-03)	0.48 ± 0.025	0.47 ± 0.025	F(1,48) = 3.138	0.08285	1
	AD (1.0e-03)	1.20 ± 0.045	1.26 ± 0.058	F(1,48) = 7.556	0.008406	0.268992
Right SMA-PUT	FA	0.42 ± 0.041	0.47 ± 0.029	F(1,48) = 20.63	3.76E-05	0.0012032 ***
	MD (1.0e-03)	0.71 ± 0.024	0.73 ± 0.034	F(1,48) = 4.459	0.03995	1
	RD (1.0e-03)	0.53 ± 0.027	0.52 ± 0.026	F(1,48) = 2.486	0.1214	1
	AD (1.0e-03)	1.07 ± 0.06	1.15 ± 0.071	F(1,48) = 16.47	0.000181	0.0057920 ***
Left SMA-PUT	FA	0.44 ± 0.041	0.46 ± 0.036	F(1,48) = 3.695	0.06052	1
	MD (1.0e-03)	0.72 ± 0.024	0.74 ± 0.033	F(1,48) = 6.4	0.01475	0.4720000
	RD (1.0e-03)	0.54 ± 0.033	0.54 ± 0.028	F(1,48) = 0.08	0.7775	1
	AD (1.0e-03)	1.10 ± 0.045	1.16 ± 0.075	F(1,48) = 10.32	0.002347	0.0751040
Right THAL-MC	FA	0.49 ± 0.031	0.52 ± 0.036	F(1,48) = 13.96	0.000497	0.0159040 ***
	MD (1.0e-03)	0.69 ± 0.018	0.70 ± 0.027	F(1,48) = 1.353	0.2505	1
	RD (1.0e-03)	0.48 ± 0.024	0.46 ± 0.025	F(1,48) = 6.618	0.01324	0.4236800
	AD (1.0e-03)	1.10 ± 0.044	1.16 ± 0.071	F(1,48) = 8.312	0.005878	0.1880960
Left THAL-MC	FA	0.47 ± 0.030	0.51 ± 0.036	F(1,48) = 17.4	0.000126	0.0040320 ***
	MD (1.0e-03)	0.71 ± 0.022	0.71 ± 0.027	F(1,48) = 0.7209	0.4	1
	RD (1.0e-03)	0.51 ± 0.027	0.49 ± 0.027	F(1,48) = 6.13	0.01687	0.53984
	AD (1.0e-03)	1.11 ± 0.042	1.16 ± 0.076	F(1,48) = 10.64	0.002037	0.0651840
Right UNF	FA	0.43 ± 0.024	0.41 ± 0.019	F(1,48) = 14.36	0.000421	0.0134656 ***
	MD (1.0e-03)	0.77 ± 0.018	0.78 ± 0.024	F(1,48) = 3.56	0.06524	1
	RD (1.0e-03)	0.57 ± 0.018	0.59 ± 0.022	F(1,48) = 13.91	0.000506	0.0161856 ***
	AD (1.0e-03)	1.11 ± 0.048	1.14 ± 0.049	F(1,48) = 2.934	0.09319	1
Left UNF	FA	0.42 ± 0.039	0.40 ± 0.024	F(1,48) = 3.973	0.05193	1
	MD (1.0e-03)	0.75 ± 0.017	0.77 ± 0.021	F(1,48) = 15.13	0.000309	0.0098720 ***
	RD (1.0e-03)	0.57 ± 0.028	0.59 ± 0.024	F(1,48) = 10.11	0.002579	0.0825280
	AD (1.0e-03)	1.18 ± 0.043	1.15 ± 0.051	F(1,48) = 4.512	0.03884	1

\*\*\* = Bonferroni corrected  $p < 0.05$  ( $0.05/32 = 0.00156$ )

CST corticospinal tract, SMA-PUT supplementary motor area-putamen tract, THAL-MC thalamus-motor cortex tract, UNF uncinate fasciculus, FA fractional anisotropy, MD mean diffusivity, RD radial diffusivity, AD axial diffusivity, SD standard deviation

putative abnormal activity in the thalamus and basal ganglia [1]. Considering the long time-course from the onset of PD-related pathology to the onset of clinical symptoms [33], the subcortical and cortical motor pathways may well have undergone compensatory and adaptive structural and functional reorganization long before PD patients have been diagnosed clinically. Such a model would be supported by our observation (Supplementary table 2) that changes in the diffusion metrics were not confined to the hemisphere contralateral to the side of dominant symptoms.

Recent evidence from PD rodent models showed axonal sprouting as compensatory mechanism [34], but this has not been studied in detail outside the nigrostriatal system. Based

on our present findings, we suggest that there may be compensatory sprouting in motor tracts in response to decreased input from the thalamus and striatum as a consequence of PD pathology. We would further suggest that sprouting should also be assessed in corticospinal and thalamo-cortical motor tracts, both in animal models and in human brains post-mortem.

### Methodological considerations

Diffusion tensor metrics are highly sensitive to white matter microstructural changes; however, they are non-specific indices with complex measures, hence one has to be cautious

when inferring any specific biological mechanisms underlying changes in these measures [35]. Before interpreting our findings in terms of putatively increased structural connections in PD we need to exclude the possibility that they are influenced by methodological artefacts. We used the dRL algorithm which reduces the number of spurious fibre orientations that can produce artefactual reconstructions of tracts and is said to be robust in mapping cortical connectivity [5]. In patient and clinical studies, presence of degeneration makes the estimated tract reconstructions prone to isotropic partial volume effects [36] but the spherical deconvolution methods make it possible to obtain accurate white matter fibres that are corrected for partial volume effects and crossing fibres. Additionally, we found a higher number of reconstructed streamlines in PD patients than in HCs in the motor tracts and the UNF even though only the motor tracts showed increased FA whereas the UNF showed decreased FA. We can thus exclude that higher FA values were driven by the increase in number of reconstructed streamlines or number of occupied voxels or tract volume.

Because FA is a normalized measure it can be affected by changes in any of the compartments of white matter. For a better understanding of the specific contributions of axonal microstructural changes and myelination to changes in the white matter architecture in PD, future studies can apply complex diffusion microstructural models such as Composite Hindered and Restricted Model of Diffusion (CHARMED) or AxCaliber [26]. However, their clinical application in patients with movement disorders is limited by the long duration of scanning protocols. Recently developed myelin water fraction mapping and quantitative magnetization transfer techniques could also be used in future studies to better quantify myelination [37].

## Conclusion

This first comprehensive deterministic tractography study of motor and non-motor tracts in PD revealed increased FA in the cortico-basal ganglia and CSTs, which may indicate compensatory mechanisms or structural changes related to altered pallido-thalamic activity in PD. We suggest that tractography be incorporated in longitudinal imaging studies of PD in order to evaluate the role of white matter changes in neurodegenerative and neuroplastic processes.

**Acknowledgments** We thank Dr Alistair Church, Dr Biju Mohammed, Dr Chris Thomas and Mrs Debbie Davies for their help with patient recruitment, and all patients, carers and control participants for their participation. We also thank Dr Nils Muhlert for his help with the subcortical volumes analysis.

The scientific guarantor of this publication is Prof. David E J Linden. The authors of this manuscript declare relationships with the following companies: Co-author Huw Morris has relationships with companies;

Abbie, Teva, UCB, Boehringer-Ingelheim, GSK, Ipsen Fund, Medtronic, MND, PSP Association. This study has received funding by: Author Jilu Princy Mole is grateful for the support from Cardiff University's Overseas Research Scholarship (2014-2017) and MRes International Scholarship (2013-2014). This study received funding from the Wellcome Trust through the Institutional Strategic Support Fund to Cardiff University. The patient data were acquired as part of the study "Real-time fMRI Neurofeedback for Treatment of Parkinson's Disease" (NCT01867827). The aging study was supported by funding from the Medical Research Council, UK, via a Clinician Scientist Fellowship to Dr. Michael J. O'Sullivan. (G0701912). This work was supported by the Swiss National Science Foundation (SNF), Switzerland (to Tobias Bracht, Grant number PBBEP3\_144797). Authors Jilu Princy Mole, Claudia Metzler-Baddeley and David E J Linden have statistical expertise in the analysis of neuroimaging data. Institutional Review Board approval was obtained. Written informed consent was obtained from all subjects (patients and controls) in this study. Some study subjects or cohorts (the controls) have been previously reported in Metzler-Baddeley, C, Jones, DK, Belaroussi, B, Aggleton, JP and O'Sullivan, M (2011). Frontotemporal connections in episodic memory and aging: A diffusion MRI tractography study. *The Journal of Neuroscience*, 31(37), 13236-13245 and Metzler-Baddeley, C, Jones, DK, Steventon, J, Westacott, L, Aggleton, JP and O'Sullivan, M (2012). Cingulum microstructure predicts cognitive control in older age and mild cognitive impairment. *Journal of Neuroscience*, 32(49), 17612-17619.

Methodology: case-control study, performed at one institution.

**Open Access** This article is distributed under the terms of the Creative Commons Attribution-NonCommercial 4.0 International License (<http://creativecommons.org/licenses/by-nc/4.0/>), which permits any noncommercial use, distribution, and reproduction in any medium, provided you give appropriate credit to the original author(s) and the source, provide a link to the Creative Commons license, and indicate if changes were made.

## References

1. Bezdard E, Gross CE, Brotchie JM (2003) Presymptomatic compensation in Parkinson's disease is not dopamine-mediated. *Trends Neurosci* 26:215–221
2. Meijer FJ, Bloem BR, Mahlknecht P, Seppi K, Goraj B (2013) Update on diffusion MRI in Parkinson's disease and atypical parkinsonism. *J Neurol Sci* 332:21–29
3. Rae CL, Correia MM, Altena E, Hughes LE, Barker RA, Rowe JB (2012) White matter pathology in Parkinson's disease: the effect of imaging protocol differences and relevance to executive function. *Neuroimage* 62:1675–1684
4. Jeurissen B, Leemans A, Tournier JD, Jones DK, Sijbers J (2013) Investigating the prevalence of complex fiber configurations in white matter tissue with diffusion magnetic resonance imaging. *Hum Brain Mapp* 34:2747–2766
5. Dell'acqua F, Scifo P, Rizzo G et al (2010) A modified damped Richardson-Lucy algorithm to reduce isotropic background effects in spherical deconvolution. *Neuroimage* 49:1446–1458
6. Phillips O, Squitieri F, Sanchez-Castaneda C et al (2014) The corticospinal tract in Huntington's disease. *Cereb Cortex*. doi:10.1093/cercor/bhu065
7. Vergani F, Lacerda L, Martino J et al (2014) White matter connections of the supplementary motor area in humans. *J Neurol Neurosurg Psychiatry* 85:1377–1385



8. Mink JW (1996) The basal ganglia: focused selection and inhibition of competing motor programs. *Prog Neurobiol* 50:381–425
9. Lindenbach D, Bishop C (2013) Critical involvement of the motor cortex in the pathophysiology and treatment of Parkinson's disease. *Neurosci Biobehav Rev* 37:2737–2750
10. Von Der Heide RJ, Skipper LM, Klobusicky E, Olson IR (2013) Dissecting the uncinate fasciculus: disorders, controversies and a hypothesis. *Brain* 136:1692–1707
11. Coenen VA, Panksepp J, Hurwitz TA, Urbach H, Madler B (2012) Human medial forebrain bundle (MFB) and anterior thalamic radiation (ATR): imaging of two major subcortical pathways and the dynamic balance of opposite affects in understanding depression. *J Neuropsychiatry Clin Neurosci* 24:223–236
12. Patenaude B, Smith SM, Kennedy DN, Jenkinson M (2011) A Bayesian model of shape and appearance for subcortical brain segmentation. *Neuroimage* 56:907–922
13. Metzler-Baddeley C, Jones DK, Belaroussi B, Aggleton JP, O'Sullivan MJ (2011) Frontotemporal connections in episodic memory and aging: a diffusion MRI tractography study. *J Neurosci* 31:13236–13245
14. Jones DK, Horsfield MA, Simmons A (1999) Optimal strategies for measuring diffusion in anisotropic systems by magnetic resonance imaging. *Magn Reson Med* 42:515–525
15. Jones DK, Williams SC, Gasston D, Horsfield MA, Simmons A, Howard R (2002) Isotropic resolution diffusion tensor imaging with whole brain acquisition in a clinically acceptable time. *Hum Brain Mapp* 15:216–230
16. (2011) Diffusion MRI: theory, methods and applications. Oxford University Press, Oxford
17. Leemans A, Jeurissen B, Sijbers J, Jones DK (2009) ExploreDTI: a graphical toolbox for processing, analyzing and visualizing diffusion MR data. Proceedings of the International Society for Magnetic Resonance in Medicine 17th Annual Meeting, Honolulu, Hawaii, 3536
18. Leemans A, Jones DK (2009) The B-matrix must be rotated when correcting for subject motion in DTI data. *Magn Reson Med* 61:1336–1349
19. Bassar PJ, Mattiello J, LeBihan D (1994) Estimation of the effective self-diffusion tensor from the NMR spin echo. *J Magn Reson B* 103:247–254
20. Pasternak O, Sochen N, Gur Y, Intrator N, Assaf Y (2009) Free water elimination and mapping from diffusion MRI. *Magn Reson Med* 62:717–730
21. Bracht T, Doidge AN, Keedwell PA, Jones DK (2015) Hedonic tone is associated with left supero-lateral medial forebrain bundle microstructure. *Psychol Med* 45:865–874
22. Smith SM, Jenkinson M, Woolrich MW et al (2004) Advances in functional and structural MR image analysis and implementation as FSL. *Neuroimage* 23:S208–S219
23. Team RDC (2014) R: a language and environment for statistical computing. R Foundation for Statistical Computing, Vienna, Austria
24. Concha L, Gross DW, Wheatley BM, Beaulieu C (2006) Diffusion tensor imaging of time-dependent axonal and myelin degradation after corpus callosotomy in epilepsy patients. *Neuroimage* 32:1090–1099
25. Lebel C, Walker L, Leemans A, Phillips L, Beaulieu C (2008) Microstructural maturation of the human brain from childhood to adulthood. *Neuroimage* 40:1044–1055
26. Assaf Y (2008) Can we use diffusion MRI as a bio-marker of neurodegenerative processes? *Bioessays* 30:1235–1245
27. Schwarz ST, Abaei M, Gontu V, Morgan PS, Bajaj N, Auer DP (2013) Diffusion tensor imaging of nigral degeneration in Parkinson's disease: a region-of-interest and voxel-based study at 3 T and systematic review with meta-analysis. *Neuroimage Clin* 3:481–488
28. Takahashi M, Ono J, Harada K, Maeda M, Hackney DB (2000) Diffusional anisotropy in cranial nerves with maturation: quantitative evaluation with diffusion MR imaging in rats. *Radiology* 216:881–885
29. Song SK, Sun SW, Ramsbottom MJ, Chang C, Russell J, Cross AH (2002) Dysmyelination revealed through MRI as increased radial (but unchanged axial) diffusion of water. *Neuroimage* 17:1429–1436
30. Budde MD, Janes L, Gold E, Turtzo LC, Frank JA (2011) The contribution of gliosis to diffusion tensor anisotropy and tractography following traumatic brain injury: validation in the rat using Fourier analysis of stained tissue sections. *Brain* 134:2248–2260
31. Winston GP (2012) The physical and biological basis of quantitative parameters derived from diffusion MRI. *Quant Imaging Med Surg* 2:254–265
32. Herz DM, Haagen BN, Christensen MS et al (2015) Abnormal dopaminergic modulation of striato-cortical networks underlies levodopa-induced dyskinesias in humans
33. Braak H, Bohl JR, Muller CM, Rub U, de Vos RA, Del Tredici K (2006) Stanley Fahn Lecture 2005: the staging procedure for the inclusion body pathology associated with sporadic Parkinson's disease reconsidered. *Mov Disord* 21:2042–2051
34. Arkadir D, Bergman H, Fahn S (2014) Redundant dopaminergic activity may enable compensatory axonal sprouting in Parkinson disease. *Neurology* 82:1093–1098
35. Jones DK, Knosche TR, Turner R (2013) White matter integrity, fiber count, and other fallacies: the do's and don'ts of diffusion MRI. *Neuroimage* 73:239–254
36. Ciccarelli O, Catani M, Johansen-Berg H, Clark C, Thompson A (2008) Diffusion-based tractography in neurological disorders: concepts, applications, and future developments. *Lancet Neurol* 7:715–727
37. Levesque IR, Giacomini PS, Narayanan S et al (2010) Quantitative magnetization transfer and myelin water imaging of the evolution of acute multiple sclerosis lesions. *Magn Reson Med* 63:633–640